Probe-based ultrahigh-density storage technology

A. Pantazi
A. Sebastian
T. A. Antonakopoulos
P. Bächtold
A. R. Bonaccio
J. Bonan
G. Cherubini
M. Despont
R. A. DiPietro
U. Drechsler
U. Dürig
B. Gotsmann
W. Häberle
C. Hagleitner
J. L. Hedrick
D. Jubin
A. Knoll
M. A. Lantz
J. Pentarakis
H. Pozidis
R. C. Pratt
H. Rothuizen
R. Stutz
M. Varsamou
D. Wiesmann
E. Eleftheriou

Ultrahigh storage densities can be achieved by using a thermomechanical scanning-probe-based data-storage approach to write, read back, and erase data in very thin polymer films. High data rates are achieved by parallel operation of large two-dimensional arrays of cantilevers that can be batch fabricated by silicon-surface micromachining techniques. The very high precision required to navigate the storage medium relative to the array of probes is achieved by microelectromechanical system (MEMS)-based ***x*** *and* ***y*** *actuators. The ultrahigh storage densities offered by probe-storage devices pose a significant challenge in terms of both control design for nanoscale positioning and read-channel design for reliable signal detection. Moreover, the high parallelism necessitates new dataflow architectures to ensure high performance and reliability of the system. In this paper, we present a small-scale prototype system of a storage device that we built based on scanning-probe technology. Experimental results of multiple sectors, recorded using multiple levers at 840 Gb/in^2 and read back without errors, demonstrate the functionality of the prototype system. This is the first time a scanning-probe recording technology has reached this level of technical maturity, demonstrating the joint operation of all building blocks of a storage device.*

Introduction

Today's wide variety of data-storage applications creates an increasing demand for high-capacity, fast-access, and low-power memory devices. The areal densities of conventional storage technologies will eventually reach fundamental physical limits, such as those due to the superparamagnetic effect in magnetic storage and the scaling limits imposed by lithography in flash memories. Therefore, new technologies are under investigation that could potentially address the future needs of data-storage applications.

Probe-based data-storage devices [1–6] are being considered as ultrahigh-density and small-form-factor alternatives to conventional data-storage devices such as the microdrive and flash memory. Probe storage relies on nanometer-sharp tips, similar to the ones used in atomic force microscopy (AFM) and scanning tunneling microscopy (STM) [7, 8], for manipulating the structure or changing the properties of materials down to the atomic scale. The use of such technologies allows densities that are far beyond 1 Tb/in^2 to be achieved. Different approaches involving materials and recording mechanisms have been investigated, such as the phase-change approach for storing information using amorphous-crystalline transitions in a phase-change medium [9, 10], the magnetic probe-based approach in which a magnetic storage medium is used and writing is achieved magnetically by means of an array of probe tips [11], and the ferroelectric approach in which information is stored using ferroelectric domains [12].

This paper focuses on a probe-storage prototype that exploits the thermomechanical method for storing and retrieving data encoded as nanometer-scale indentations in thin polymer films [5, 6]. Thermomechanical writing was originally investigated in [13]. Recently, experimental results using single probes have shown that with the thermomechanical write/read process, data can be recorded at a density of 641 Gb/in^2 and read back with

0018-8646/08/$5.00 © 2008 IBM

raw error rates better than 10^{-4} prior to error-correction coding [14]. Moreover, using advanced polymer media and the same recording method, a feasibility study has shown that densities of 4 Tb/in^2 can be achieved [15].

Single probes are relatively slow in writing and retrieving data compared to conventional techniques. High data rates are possible by operating large arrays of probes in parallel, with each probe performing read, write, and erase operations on an individual storage field. A first large two-dimensional (2D) array of 1,024 (32×32) cantilevers with integrated tips and sensors has been successfully fabricated using silicon micromachining techniques [16]. More recently, a new interconnect technology for integrating the cantilever array with the CMOS (complementary metal-oxide semiconductor) analog front-end (AFE) chip has been developed [17]. In this approach, the cantilever array is transferred and interconnected to its CMOS AFE counterpart chip on a full wafer-to-wafer basis, thereby overcoming the challenge of connectivity to the driving electronics that is encountered in the parallel operation of large cantilever arrays.

In probe systems, the rotating-disk and single-head-per-surface paradigm of hard-disk drives has been abandoned in favor of microelectromechanical system (MEMS)-based x and y actuators that position the storage medium relative to the array of probe tips for parallel write and read operations [18]. Typical actuation distances are on the order of 100 μm. Moreover, in addition to x and y actuators, positioning sensors are required with a dynamic range of approximately 100 μm and displacement resolution of less than approximately 1 nm.

We have built a small-scale prototype storage system based on arrays of scanning probes with complete servo-navigation and parallel write and read functionality, and we have demonstrated multiple-sector writing and reading with eight probes in parallel at a record areal density of 840 Gb/in^2 and a raw bit error rate of approximately 10^{-4} prior to error-correction coding. This is the first time a scanning-probe recording technology has reached this high level of technical maturity, demonstrating the joint operation of all building blocks of a storage device based on local-probe techniques. The storage system encompasses 1) a MEMS assembly comprising a cantilever array chip and a microscanner carrying the storage medium, 2) an integrated analog CMOS front-end chip driving the cantilever array, 3) a novel poly-aryl-ether-ketone (PAEK)-based ultrahigh-temperature polymer used as storage medium, and 4) a new navigation system based on medium-derived positioning information that achieves an ultrahigh positioning resolution during reading and writing, as well as 5) a servo controller for subnanometer positioning during device formatting.

The remainder of this paper is organized as follows. First, we describe the thermomechanical probe-storage system, along with the primary challenges. A description of the components of the MEMS storage device is then given. Next, we discuss the system aspects of the storage system. Experimental validation of the prototype operation with a sector write/read demonstration is also presented.

Thermomechanical probe-storage system

In thermomechanical probe-based storage, information is stored as sequences of indentations written on thin polymer films using a 2D array of AFM cantilevers. The presence or the absence of indentations corresponds to logical 1s or 0s, respectively. Each cantilever performs read, write, and erase operations in an individual storage field with an area on the order of 100 μm $\times$ 100 μm. The tip–medium spacing is controlled globally, and the write and read operations depend on mechanical x and y scanning of the storage medium. High data rates are possible by parallel operation of all or a subset of the cantilevers.

Thermomechanical writing is performed by applying an electrostatic force through the cantilever to the polymer layer and simultaneously softening the polymer layer by local heating. A heater integrated into the cantilever directly above the tip is heated to a relatively high temperature of about 400°C. The heat is transported from the heater through the tip and into the polymer medium under the tip apex [19]. For readback sensing, a second heater placed beside the tip is heated to a temperature in the range of 150–300°C. The principle of thermal sensing exploits the fact that the thermal conductance between the resistive heater and the storage substrate changes as a function of the distance between them [20]. The medium between the resistive heater and the storage substrate, which in our case is air, transports heat from the cantilever to the substrate. When the distance between the cantilever and the substrate decreases as the tip moves into an indentation, the heat transport through the air becomes more efficient, resulting in a change of the cantilever temperature. Because the electrical resistance of the heater depends on its temperature, the value of its resistance decreases when the tip moves into an indentation. Under typical operating conditions, the sensitivity of thermomechanical sensing, determined by the relative variation of the heater resistance $\Delta R/R$, is approximately 10^{-4} for a distance change of 1 nm. The speed of this thermomechanical reading process is limited by the thermal time constant of the heater, which is on the order of a few microseconds. As mentioned above, one solution to achieve competitive

data rates is to simultaneously access all or a large subset of the cantilevers in the 2D array.

An important component of the probe-based storage system is the miniaturized scanner with x and y motion range that is on the order of the pitch between the cantilevers in the array. To generate information about the position of the microscanner, two pairs of thermal position sensors are included in the cantilever array. The cantilever array, the AFE chip, and the microscanner constitute the MEMS assembly shown in the schematic diagram of the probe-storage system in **Figure 1**.

Another component of a probe-storage device is the positioning and navigation unit with its sub-nanometer precision requirements and the read channel, which is associated with the multisensor cantilever array. Finally, the dataflow component includes the higher system-level functionality needed to interface the multiple storage fields with a host device. The high parallelism of the storage fields requires development of new dataflow architectures to increase the error-correction capability and reliability of the system. The system block diagram shown in Figure 1 depicts the main system-related aspects of the thermomechanical probe-storage device and includes the servo controller, the read channel, and the dataflow.

Device description and identification

The MEMS assembly, in a form factor that is compatible with most memory cards (16.5 mm × 17.5 mm × 0.8 mm), consists of the microscanner, a silicon baseplate, and the cantilever array chip. The microscanner consists of a 6.8-mm × 6.8-mm scan table and a pair of voice-coil-type actuators, all of which are supported by springs [18]. The mechanical components of the microscanner are fabricated from a 400-μm-thick silicon wafer using a deep-trench etching process. This microscanner is then mounted on a silicon baseplate that acts as the mechanical ground of the system. The scan table, which carries the polymer storage medium, can be displaced in two orthogonal directions, namely x and y, in the plane of the silicon wafer. Each voice-coil actuator consists of a pair of permanent magnets glued into a silicon frame, with a miniature coil having a resistance of 8.4 Ω mounted between them on the baseplate. The cantilever array chip is fabricated using the lever-transfer technique [17]. The microscanner is mounted on the cantilever array with spacers that are fabricated on both the microscanner and the array chip. These spacers have been designed to achieve a spacing of 550 nm between the cantilever tips and the medium, which is spin-coated on the scan. The tip–medium distance for each cantilever also depends on the cantilever bending uniformity within the array, as discussed in the following section.

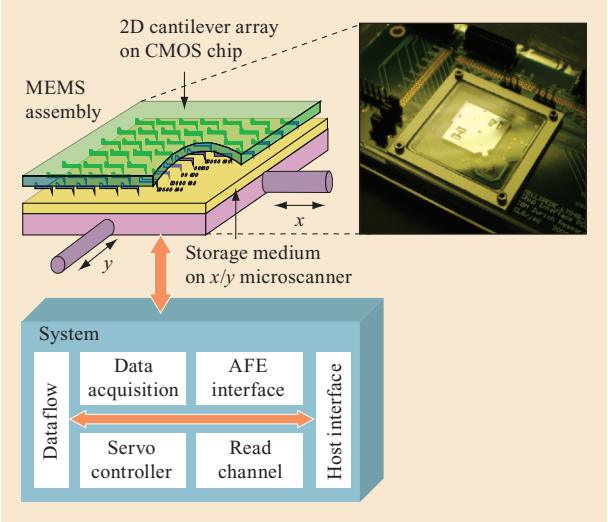

Figure 1

Architecture of the prototype system. The MEMS assembly includes the cantilever array and CMOS chip (green), the storage medium (yellow), and microscanner (pink). (MEMS: microelectromechanical system; CMOS: complementary metal-oxide semiconductor; AFE: analog front end.)

Cantilever array

A large 2D array consisting of up to 4,096 (64 × 64) cantilevers with integrated tips and sensors has been successfully fabricated using silicon micromachining techniques [17]. Each cantilever is of a three-terminal design, with separate resistive heaters for reading and writing and a capacitive platform for enhanced electrostatic force. The fabrication process is based on a new approach in which the cantilever array is transferred and interconnected to its CMOS counterpart chip on a full wafer-to-wafer basis [17]. The AFE design supports the parallel write and read operations of the cantilevers in the array [21, 22]. Specifically, at the input of each cantilever channel is a high-voltage switch matrix that selects the actual operation of the respective cantilever (read, write, or inactive). To perform parallel write and read operations, the switch matrix is configured to enable the application of the electrostatic force and the heating at the selected cantilevers. The other cantilevers are set in the inactive mode, during which the circuitry is designed to keep them at the same potential as the silicon substrate coated with the storage medium. This will prevent pull-in of the cantilevers to the surface.

For parallel operation of the cantilevers, the tip–medium distance is important because it determines the loading force of each cantilever while in contact with the medium. Therefore, the cantilever bending uniformity is of paramount importance for the performance of the

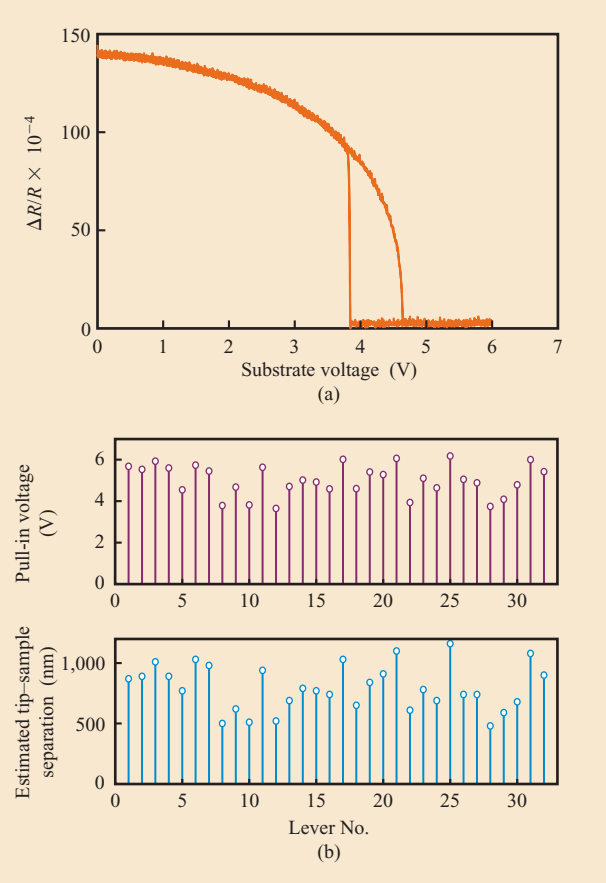

Figure 2

Cantilever array: (a) typical force-curve measurement; (b) pull-in voltage and estimated tip–medium distance for 32 cantilevers of the array. The phrase *force curve* for (a) arises from the increased force due to the increasing voltage indicated along the x-axis. $\Delta R/R$ provides an indication of relative resistance.

parallel write and read process. Because the cantilever array is mounted at a fixed distance from the medium surface, each cantilever can come into contact with the medium by applying an electrostatic force. Therefore, a measure of the bending uniformity is the voltage needed for each cantilever of the array to come into contact with the polymer medium. **Figure 2(a)** schematically shows a typical force-curve measurement. Starting from the rest position of the cantilever, the negative voltage on the silicon substrate coated with the storage medium is increased, and the cantilever moves toward the substrate until the tip comes into contact with the storage medium. As the voltage is further increased, the tip remains in contact with the medium, and a higher loading force is exerted. Afterward, the cantilever is retracted by reducing the force until the tip snaps off the surface and returns to its initial position. The measurement of interest is the voltage required on the substrate so that the tip comes into contact with the medium. Assuming the cantilever spring constants are approximately equal, the variation of the pull in voltage of the cantilever provides a measure of the cantilever bending uniformity. **Figure 2(b)** shows the pull in voltage calculated by the force-curve measurements of the 32 cantilevers in the array, which yields a mean value of 5 V and a standard deviation of 0.75 V. The same figure shows the tip–sample separation estimated from the measured cantilever bending. From the uniformity measurements, a standard deviation of 180 nm is calculated. Also, as shown in the figure, there is a strong correlation of the tip–sample separation estimates with the measured pull in voltages.

Microscanner

The microscanner consists of a scan table, which carries the storage medium, and two voice-coil-type actuators. Each voice-coil actuator consists of a pair of permanent magnets mounted on a shuttle, with a miniature coil mounted between them on the baseplate. Actuation in the x- or y-direction is achieved by applying a current to the x or y coil, which generates a force on the magnets and induces a displacement of the shuttle. This motion is coupled to the scan table by means of a mass-balanced pivot scheme that translates the motion of the shuttle to the scan table and makes the microscanner robust against external shock and vibrations. By balancing the masses on each side of the pivot, the forces from an external acceleration on the scan table and actuator side cancel each other, leaving the microscanner largely immune to external influences [18].

The microscanner can be regarded as a two-input, two-output system that relates the input coil currents (in milliamperes [mA]) to the output displacements (in micrometers [μm]) in both x- and y-directions of actuation. In order to identify the transfer functions that describe this system, the frequency responses of the microscanner in the x- and y-directions are obtained using the position information from the thermal sensors in the range from 1 Hz to 10 kHz. The experimentally obtained frequency responses in both directions are shown in **Figure 3(a)**. As can be seen, the dynamics are dominated by the first resonance mode, which can be accurately captured by a simple mass-spring-damper second-order model. The frequency response of the x-direction has a resonance frequency at 175 Hz, and the frequency response of the y-direction has one at 158 Hz. The quality factors, which involve a measure of the resonant peak (or equivalently a measure of the damping), are 14.5 and 17.8 for the x-direction and the y-direction, respectively. In the higher frequency regime, the microscanner frequency response exhibits higher-order resonance modes. It was also found that these

higher-order resonances change with the x/y position, which further complicates an exact modeling of the microscanner.

Another important characteristic that describes the motion of the microscanner is the cross-coupling between the axes. **Figure 3(b)** shows the typical cross-coupling on the y-axis due to x-motion for various values of the displacement in the y-direction. As shown in Figure 3(b), the cross-coupling is nonlinear and position dependent. The experimentally obtained frequency responses for each direction and the cross-coupling data can be used to create a microscanner model for controller design and simulation purposes [23].

Thermal position sensor

Two pairs of thermal position sensors are used to provide x/y position information of the microscanner to the servo controller. The sensors consist of thermally isolated, resistive strip heaters made from moderately doped silicon [24]. Each sensor is positioned above the edge of the scan table and heated to a temperature of about 100°C. A fraction of this heat is conducted through the ambient air into the scan table, which acts as a heat sink. Displacement of the scan table translates into a change in the cooling efficiency and hence a change in the temperature of these heaters. This change in temperature can be measured as a change in electrical resistance. Because the sensors are driven with a constant voltage, these changes in resistance can be detected by measuring the resulting current. In order to minimize drift effects, the sensors are operated in pairs using a differential configuration.

The behavior of the thermal position sensors in terms of sensing bandwidth and noise is important for the performance of the closed-loop system. The thermal sensor bandwidth—that is, the −3-dB cutoff frequency of its sensing transfer function—is determined by the thermoelectric response of the heaters [25, 26]. The sensing transfer functions can be identified for both thermal position sensors and at different microscanner positions. The measurements have shown that the sensing transfer function of each position sensor can be well approximated by a first-order response whose bandwidth varies as a function of the microscanner position.

Figure 4(a) depicts the behavior of both thermal position sensors. Ideally, for a linear sensor, the bandwidth would have been invariant across the travel range of the microscanner. This nonlinear behavior of an individual thermal sensor can be explained by the large change in overlap due to the motion of the microscanner. As mentioned, the sensors are operated in a differential configuration to increase the signal-to-noise ratio and reduce drift effects. The bandwidth calculation for the

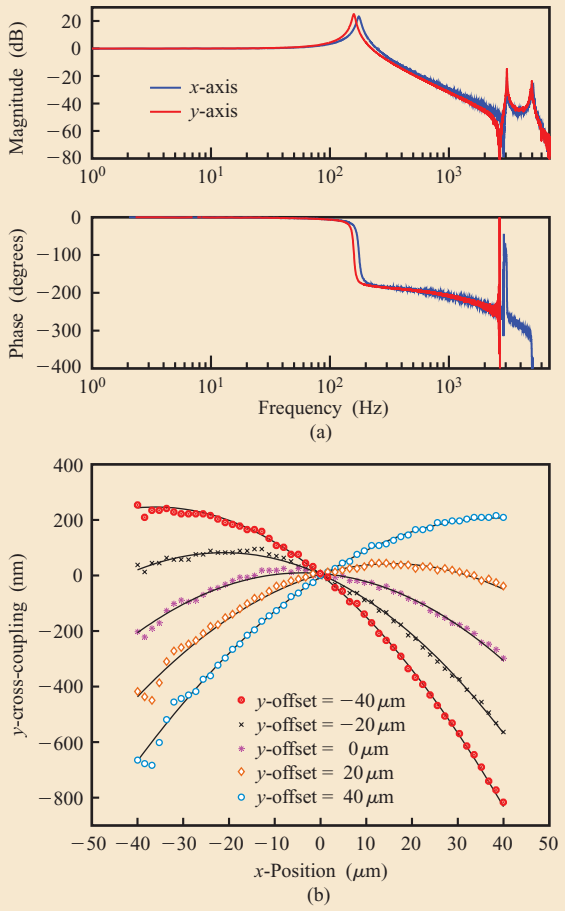

Figure 3

Microscanner: (a) measured frequency responses in the x- and y-directions; (b) measured cross-coupling between the x- and y-axes. (From [23]; ©2007 IEEE.)

differential configuration shows that the latter is quite linear and can be approximated by a first-order response with a bandwidth of approximately 4 kHz.

Positioning accuracy is related to the intrinsic noise characteristics of the sensors. The total measurement noise comprises the thermal position sensor noise and the quantization noise from the 16-bit analog-to-digital converters used. A typical measurement of the standard deviation of the thermal sensor noise is about 0.8 nm in a 10-kHz bandwidth. Although the accuracy of the sensor is reasonably good, there is a significant low-frequency component, as can be seen from the power spectral density of the sensor noise shown in **Figure 4(b)**. The dominant noise source in thermal sensing is $1/f$ noise, which depends on the number of carriers, as well as the thermal noise of the silicon resistor.

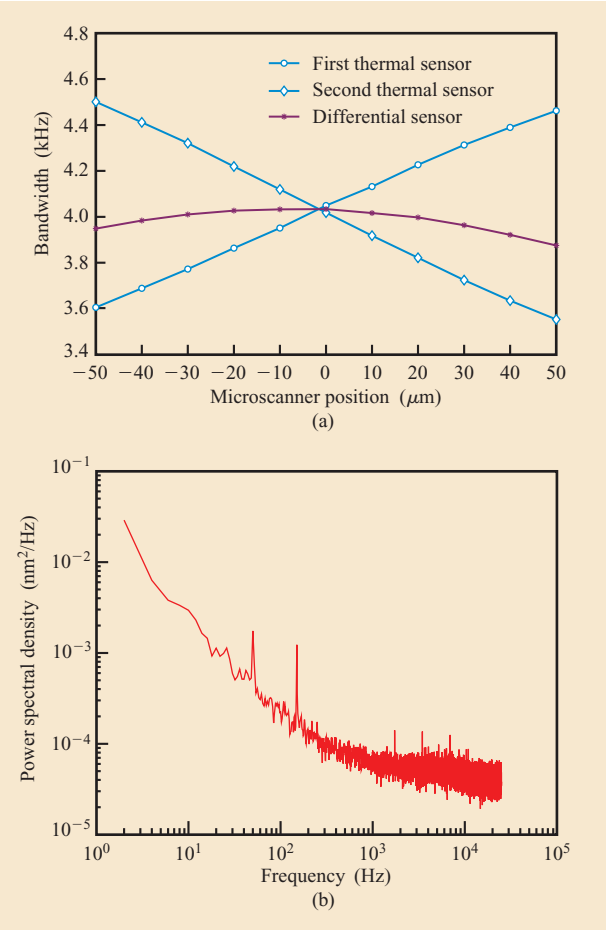

Figure 4

Thermal position sensor: (a) measured bandwidth as a function of microscanner position; (b) measured noise power spectral density.

Polymer medium

The polymer medium plays a crucial role in thermomechanical data storage. The rationale behind the polymer medium design relates to basic physical principles underlying the formation of nanoscale indents. When an indent is written, the medium is in essence elastically deformed, and the deformation is locked by the discrete nature of monomer reconfigurations within the polymer backbone, termed α-transitions. The α-transition activity can be enhanced by applying thermal and mechanical energy during writing, which renders the polymer easily deformable. At the end of the write event, the heat and the pressure are turned off within less than 1 μs, causing the activity to slow down by orders of magnitude, thereby locking the indent in its deformed state. This kinetic switching provides the memory function of the polymer medium. However, the indent representing a bit is a metastable object [5]. The mechanical stress associated with the deformation provides a restoring driving force, but the relaxation is kinetically hindered by the slow α-activity. It is important to note that the writing of an indent does not involve irreversible processes such as the breaking of chemical bonds or the diffusive motion of polymer chains.

The essential criteria for a polymer storage medium are low-mechanical-stress writing conditions in order to minimize tip wear, thermal and mechanical robustness in order to prevent chemical degradation, and repeated erasability of written indentations. These rather straightforward requirements contrast with the huge space spanned by parameters that influence the thermomechanical properties. Tip temperature, indentation force, and heating and loading times can be controlled for a given tip–medium combination. The shape, radius, and opening angle of the tip, as well as the chemical composition of the polymeric storage medium, including cross-linking, are additional parameters [19, 27, 28]. Despite the complexity, a small number of design rules have been identified as being crucial for the polymer media. First, the glass transition temperature, which sets the temperature scale for the α-transition activity of the material, should be in the range 150–190°C, the lower bound being dictated by bit retention requirements and the upper bound being dictated by low-stress writing conditions. Second, a high degree of cross-linking (chemical bonds between polymer chains) is needed in order to be able to write and erase the same bit for thousands of times and to preserve the shape of the bit during read operation. Cross-linking constrains the mobility of the polymer chains by providing a firm interconnection network that effectively suppresses diffusive motion [29]. The network also acts as an elastic matrix enhancing the erase functionality by furnishing a well-defined restoring force. Third, the polymer should be thermally stable, enabling one to use high-temperature, low-force writing conditions, which are favorable for minimizing tip degradation and indent relaxation. Finally, a parameter known as the *yield activation energy*, which describes the energy barrier associated with the α-transitions, must be greater than approximately 4 eV in order for thermally activated relaxation to be sufficiently slow such that the data can be retained for more than 10 years at 85°C, as is required for a typical portable device. It may appear surprising that the last requirement can be met at all with polymers.

Poly-aryl-ether ketones provide a particularly well-suited polymer system for our purposes by combining excellent thermal stability with the ability to tune the glass transition temperature and cross-link density over a wide range. The polymer medium used in this study had a targeted molecular weight of 4,000 and incorporated diresorcinol in the backbone and ethynyl groups for

cross-linking functionality. The glass transition temperature was in the targeted range, and the yield activation energy was empirically determined to be on the order of 5 eV. By fine-tuning the cross-link density, more than 2,500 erase cycles were experimentally demonstrated at 1 Tb/in^2. No loss of signal quality was observed in these experiments, suggesting that substantially more cycles are possible, yet not experimentally confirmed because of technical limitations requiring months of continuous observation in order to extend this limit by another order of magnitude. Another critical issue is the endurance of the written information as a function of time and repeated reading events with the same tip. Endurance and wear studies are predominately conducted using experimental test stands with piezo-scanners and single cantilever functionality [19, 27, 28]. It was experimentally demonstrated that one and the same bit can be repeatedly read at least 2×10^5 times without loss of signal quality and that the tip is able to sustain 700 m of travel corresponding to the reading of 5×10^{10} symbols at 1 Tb/in^2. Note that also here, the limits are given by the duration of the experiment and not by the material limitations. An experiment demonstrating the repetitive reading of the same track over a period of 3 months is shown in **Figure 5(a)**. This experiment was performed on the prototype system that offers the additional flexibility of being able to locate the same position with nanometer accuracy. In the first month, we conducted four experiments with the tip reading approximately 1.5×10^7 symbols. Another two experiments were conducted during the next 2 months with the tip reading in total approximately 2.5×10^7 symbols. Note that between experiments, no reading or writing operations were performed. As shown in Figure 5(a), aside from an initial small relaxation of the indentations, the average value of the measured bit depth is not reduced over time and with repetitive reads.

Other important characteristics that affect the performance of the prototype system are medium noise and indentation depth. Medium noise manifests itself in the readback signal as variations of the nominal signal amplitude. It originates from the storage medium structure that is not perfectly flat but exhibits finite surface roughness. On the other hand, the indentation depth affects the signal amplitude level. However, at high storage densities, variations on the signal amplitude level occur because of a nonlinear interaction mechanism between indentations, called *partial erasing* [30]. Specifically, in thermomechanical writing on polymers, the creation of a new indentation too close to an existing one can result in a partial erasing of the existing indentation. The recording performance can be characterized using the signal-to-distortion ratio (SDR), which quantifies the influence of all the distortions on the readback signal. The SDR depends on the indentation depth, measured by the average amplitude levels of 0s and 1s, as well as on the variance of the total distortion, that is, the deviations around the average amplitude levels.

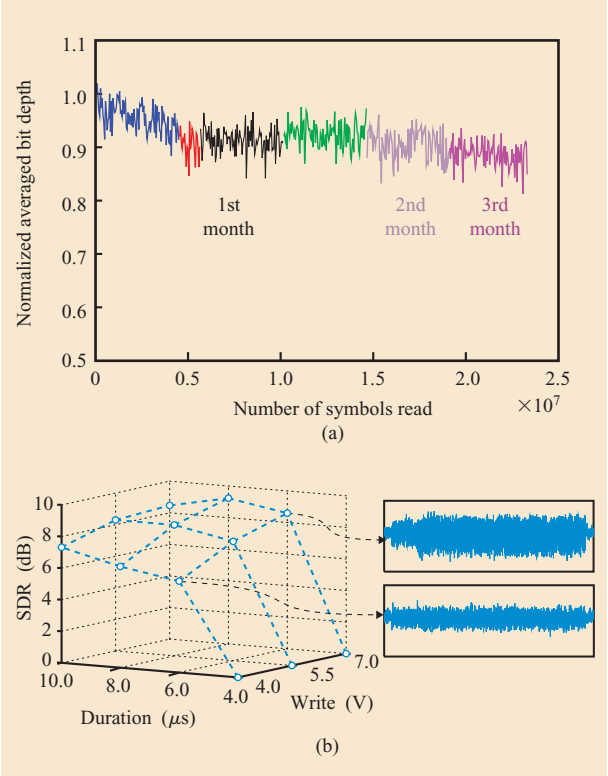

Figure 5

Polymer medium: (a) repetitive reading of the same track over a period of 3 months at 840 Gb/in^2. Each color corresponds to a reading at different time instants. For example, in the first month, we conducted four experiments at different time instances. (b) Measured signal-to-distortion ratio (SDR) for different operating conditions at 840 Gb/in^2.

The overall recording performance depends on the writing parameters such as heater temperature, applied force, and heating time. In order to investigate how the recording performance depends on the operating parameters, random data were recorded with various parameter sets, and the SDR was calculated from the captured readback signals. **Figure 5(b)** shows the measured SDR in decibels as a function of the write voltage on the cantilever and the heating time. The readback signals used to calculate the SDR are shown for two cases. Specifically, in this experiment, the loading force was kept constant while the applied voltage, which predominately affects the heater temperature, was varied from 4 to 7 V and the heating pulse duration varied from 4 to 10 μs. It can be seen that the recording performance

strongly depends on the amplitude and the duration of the applied voltage. Below certain values, no indentations can be obtained; above a certain threshold, the performance increases when either the amplitude or the duration of the applied write pulse is increased. For high storage densities, further increases in the operating conditions result in increasing the nonlinear partial erasing effects between adjacent bits. Other parameters, such as the loading force, have similar effects, as expected. The SDR measure can be used to characterize the effect of the operating parameters of the system on the recording performance.

System aspects

From a system point of view, a probe-storage device comprises a servo controller for navigation and nanopositioning, a read channel including the data and servo detectors, and the dataflow encompassing the modulation and error-correction functionality. The servo controller uses the positional information obtained from the thermal sensors and from dedicated fields on the storage medium to derive the control signals for the electromagnetic coil actuators of the microscanner [23]. The main challenge for the servo controller is the extreme precision in navigating the probe tips to the desired position that is required for ultrahigh-density data storage. The data read channel is responsible for retrieving the information from the readback waveform of the thermomechanical recording channel [30]. Effective detection schemes are needed to enhance the recording performance in the presence of signal distortions and nonlinearities at high storage densities. Finally, the dataflow includes all functions related to the host interface, that is, error-correction coding, constrained coding, data formatting, and interleaving. The flexibility offered by the large number of probes that operate in parallel can be exploited at the system level to increase the error-correction capability, the storage efficiency, and the reliability of the system. The system components are described in the following sections.

Position error signal and servo channel

The thermal position sensors can provide high-precision measurements of the microscanner position but tend to suffer from low-frequency drift. Therefore, a control scheme relying on the thermal sensors alone is not suitable for long-term operation of the device. An alternative medium-derived position error signal (PES) can be obtained by reading prewritten servo patterns on dedicated servo fields. These servo fields are a small number of storage fields that are reserved exclusively for servo-control purposes. The approach for PES generation is based on the concept of vertically displaced bursts, arranged in such a way as to produce two signals in quadrature that guarantee a uniquely decodable PES, that is, each PES value is mapped to a unique cross-track position [6]. Therefore, the medium-derived PES accurately captures deviations from the track centerline for each data track.

Medium-derived PES can be generated using the servo burst configuration illustrated in **Figure 6**. The A, B, C, and D bursts are written in four different servo fields. Servo bursts labeled A and B are used to create the in-phase signal (I), and C and D to create the quadrature signal (Q). The cross-track distance between indentation centers of the same burst is equal to the track pitch (TP), whereas the distance between indentation centers in bursts A and B (or C and D) is $TP/2$. The distance between A and C is $TP/4$. The track centerlines of the data fields coincide with the centers of servo burst C. For PES generation, a parallel read operation of the four servo fields is performed while scanning in the x-direction. The amplitude of the readback signal depends on the position of the tip relative to the recorded surface at the time of reading. The readback signal is strongest when the tip is positioned exactly over the center of the written indentation. As the distance of the tip from the indentation center increases, the readout signal strength decreases, reaching a minimum level when the tip is away from the indentation. To generate the PES, four samples of the readback signal for each written indentation are used for correlation with a pulse shape representing a typical indentation and for estimating the indentation depth. The oversampling of four samples is used to minimize the impact of timing imperfections on the system. To reduce the effect of noise on the PES, the estimated indentation depth values are then filtered. The average values $\bar{A}$, $\bar{B}$, $\bar{C}$, and $\bar{D}$, corresponding to bursts A, B, C, and D, are then used to calculate the in-phase signal as the difference $\bar{B} - \bar{A}$ and the quadrature signal as the difference $\bar{D} - \bar{C}$. Note that the quadrature signal exhibits zero crossings at the points where the in-phase signal has local extrema. The final PES is generated by combining the two signals (I and Q) and has zero crossings at all track center locations, and an almost linear range between $-TP/2$ and $TP/2$. The medium-derived PES provides y-positional information around the track centerline and, therefore, has a maximum range of TP. Unlike the thermal position sensor, the medium-derived PES does not suffer from low-frequency noise.

Servo controller

The main function of the servo controller in the MEMS-based storage system is to ensure accurate positioning of the probes over the storage medium so that data tracks are uniformly written and read back with sufficient accuracy to guarantee a low error rate. As the areal density of the system is increased to the terabit-per-

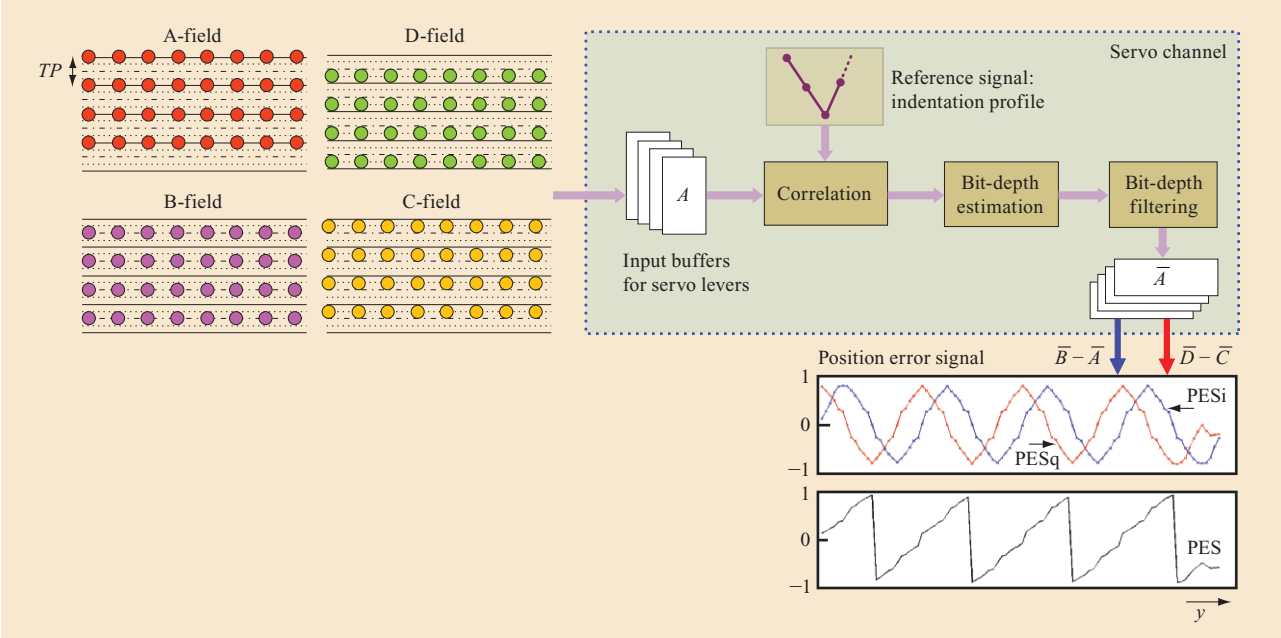

Figure 6

Position error signal and servo-channel configuration. (TP: track pitch; PES: position error signal.)

square-inch regime and beyond, the performance requirements for the servo system become very stringent. In general, the servo system in such a storage device has two functions. First, it locates the target track to which information is to be written or read back from, starting from an arbitrary initial position of the scan table carrying the storage medium. This is achieved by the seek-and-settle procedure. Because actuation distances typically are on the order of 100 μm and the components have small masses, the positioning delays are much smaller than in disk drives. Experiments have yielded remarkably short seek times, on the order of 1 ms for the worst-case seek operation [23, 31]. The second function of the servo system is to maintain the position of the read/write probes on the center of the target track while scanning along the length of this track. This is achieved by the track-follow procedure. During the track-follow procedure, each track is scanned in the horizontal direction with constant velocity while maintaining the fine positioning in the cross-track direction in the presence of disturbances and noise. At the end of each track, a short seek operation is used to move to the next track [32]. In addition to the two main servo functions needed in a normal device operation, the servo information yielding the medium-derived PES must be written in the servo fields prior to using the MEMS storage device. Precise writing of these servo fields is of great importance for reliable operation of the storage device. Servo controllers that provide such subnanometer precision have been designed for this purpose.

In the prototype system, track-follow control along the scanning direction (x-direction) is based solely on the thermal position sensor information. In contrast, the track-follow controller for the y-direction employs both the global position information from the thermal sensors and the medium-derived PES. There are separate controllers for the x- and y-motion of the microscanner, each one consisting of a linear quadratic Gaussian (LQG) regulator, a tracking controller, notch filters, and a feed-forward component. The control architecture depicted in **Figure 7** shows a block diagram of the feedback loop for one direction of motion. In this figure, P denotes the dynamics of motion of the microscanner in one direction and S represents the dynamics of the thermal sensor. Furthermore, r is the reference signal and y stands for the motion of the microscanner. The variables d_i, d, and n denote the input disturbance, the output disturbance, and the noise signals, respectively. A set of notch filters, N_F, is incorporated into the feedback loop to minimize the effect of the higher-order resonances of the microscanner. The feed-forward component, K_{FF}, is selected to be equal to the inverse of the dc gain of P to achieve better tracking performance. The tracking controller has a two-input one-output structure and can be described by a transfer function K_I from the thermal sensor error signal to the output and a transfer function K_{II} from the PES to the

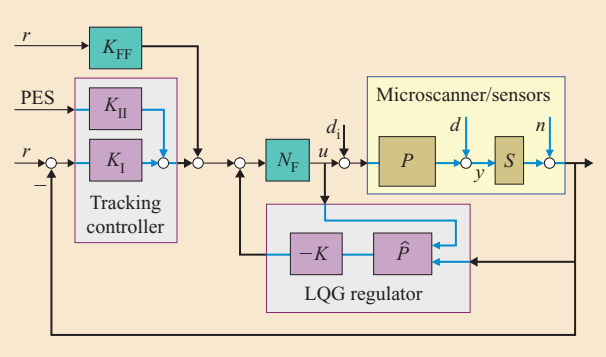

Control architecture. Here, u is the control current. $\hat{P}$ indicates a model estimating the response of the microscanner (P). The minus sign near the bottom left arrowhead indicates a subtraction operation for the signal. (LQG: linear quadratic Gaussian.)

output. For the x-direction, no medium-derived PES information is available; therefore, this signal is set to zero, and control is based exclusively on the thermal position sensors.

The primary purpose of the feedback controller in the x-direction is to maintain a constant velocity while writing and reading information. This requirement can be translated into the ability of the closed-loop system to track the reference signal, to mitigate the effect of external shocks and vibrations, and to reduce the effect of sensor noise on the position of the microscanner. A detailed analysis based on closed-loop transfer functions is given in References [23] and [33]. From the transfer function analysis, a reference tracking bandwidth of more than 1 kHz and a rejection capability for disturbances of up to approximately 300 Hz have been shown. From the noise sensitivity transfer function and the thermal sensor noise characteristics described in the previous section, the impact of measurement noise to the system can be estimated [33]. The standard deviation of the estimated microscanner perturbation due to measurement noise was found to be about 0.7 nm [34]. It has been verified that these nanometer-scale microscanner perturbations while scanning in the x-direction are the primary source of the timing jitter in the readback signal [34]. The error rate performance of the storage device depends on the amount of timing jitter in the readback signal. Therefore, the accuracy of the thermal position sensors and the noise sensitivity characteristics of the closed-loop system are crucial parameters determining the reliability of the high-density storage system.

The main purpose of the feedback controller in the y-direction is to maintain the position of the probes on the track centerline while writing and reading from a specific track. Deviations of the probes from the track centerline result in signal-to-noise ratio (SNR) loss in the readback signal. The challenges for the y-controller originate from the disturbance-rejection requirements and the low-frequency noise characteristics of the thermal sensor signal. In addition to external shocks and vibrations, the feedback loop must mitigate the disturbances that originate from cross-coupling in the y-position due to the scanning motion in the x-direction. In a control scheme based solely on thermal sensor information, drift and low-frequency sensor noise may cause deviations from the track centerline. To address this problem, the y-axis feedback loop employs both the global-position information from the thermal sensors and the medium-derived position information in a two-sensor-controller configuration. With the *a priori* knowledge of the noise characteristics of both sensors, the controller can be designed such that the positional information from the medium-derived PES is primarily used for control at low frequencies. References [23] and [35] present a novel control architecture based on the H_∞ control framework that uses the best measurement in different frequency regions. For the small-scale prototype, an alternate suboptimal two-sensor scheme was developed and implemented. This scheme is illustrated in Figure 7, where estimation and regulation are based only on the thermal sensor signal, as in the case of the x-direction control. The frequency separation in this scheme is assigned to the tracking controller, which is different for each of the sensors. The final positioning error is a combination of the individual contributions of each sensor. Using the closed-loop transfer functions, the standard deviation of the total y-positioning error has been estimated to be approximately 0.6 nm, which is expected to be within the tolerable limits.

Data read channel

In this section, we describe the read channel implemented for each cantilever. The complete read signal path consists of the read/write physical process and the data read channel. The read channel consists of an analog electronics part (also called the *analog front end*) and a digital part, as illustrated in **Figure 8**. In this figure, a model of the read signal path is shown, in which the channel input symbols are denoted by a_k and the continuous readback signal by $r(t)$. By modulating an underlying write pulse represented by the delta function $\delta(t)$, the sequence of channel input symbols is transformed into a continuous-time write signal, which is used to store the information in the medium. When the stored information is read back, the signal obtained is a distorted version of the corresponding write signal. This distortion is the result of the combined action of the write and read processes and is represented by the storage

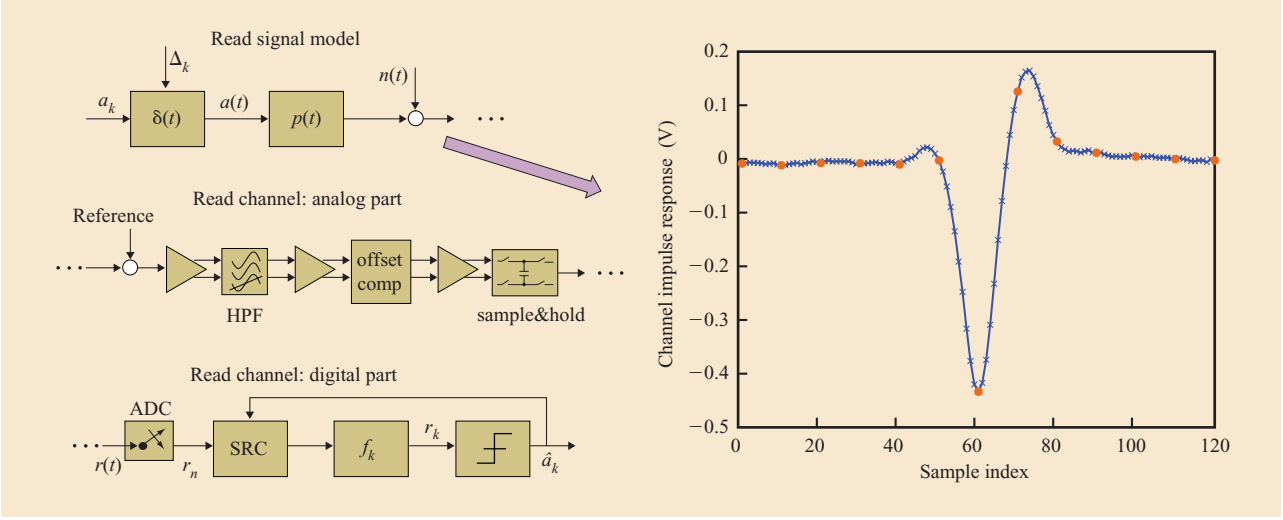

Figure 8

Data read channel. (HPF: high-pass filter; offset comp: offset compensation.) (Data curve from Reference [34]; ©2007 IEEE.)

channel. The typical channel in probe storage resembles a truncated sinc function but is not necessarily symmetrical around the main lobe. Figure 8 depicts a channel response that has been extracted by least-squares fitting of a heavily oversampled, experimentally obtained readback waveform with a symbol spacing of 20 nm. The readback signal is corrupted by noise and distortions of various forms. Two primary noise sources exist: 1) electronics and head noise and 2) medium noise. The former is usually a combination of an additive white Gaussian noise process with a $1/f$ component, and the latter is modeled as an additive colored Gaussian process. This choice was validated by an extensive analysis of experimentally obtained readback waveforms, which revealed that medium noise exhibits rapid roll-off at high frequencies and is Gaussian distributed. In the diagram of Figure 8, $n(t)$ denotes the combined contribution of electronics and medium noise.

The two significant sources of distortion in the readback signal are read and write jitter. Write jitter arises from deviations in the actual positions of the write pulses with respect to their intended positions. It can be modeled by a random deviation in the position of the write pulses and is represented by Δ_k in Figure 8. Read jitter can be modeled as random deviations of the sampling instants from their nominal temporal positions. There are several possible sources of read/write jitter. Characterization of the random nanometer-scale perturbations of the microscanner has shown that these random perturbations are the predominant source of read/write jitter [34].

The analog part of the read channel is implemented in the integrated AFE CMOS chip that includes the complete circuitry to support parallel operation of the cantilevers [21, 22]. The design of the on-chip read-channel circuitry allows reliable detection of the tiny signal current obtained with the thermal sensing scheme ($\Delta R/R < 10^{-3}$ for a typical indentation). This small sensitivity of the thermal sensing scheme leads to a large offset current. Therefore, the information-carrying signal can be viewed as a small signal superimposed on a very large offset. The bulk of this offset is canceled by means of an identically biased reference element directly in the input stage of the AFE chip to minimize power. The current from the input stage is converted to a differential voltage signal. A high-pass filter is then used to remove the remaining bias current and low-frequency noise but can be bypassed during calibration. Two instrumentation amplifiers with programmable gain and bandwidth ensure the flexibility necessary to adapt the transfer function of the front end to a wide range of operating conditions. An additional offset-compensation stage between the second and third amplifier is used to cancel the input offset of the amplifiers in high-gain configurations. A sample-and-hold stage is used to synchronously sample all data channels before the outputs are sequentially multiplexed to the ADC (analog-to-digital converter).

In the digital domain, the sequence at the output of the ADC is first synchronized to the symbol rate. This is accomplished through a timing recovery loop and an interpolator, which are schematically represented by the sampling rate converter (SRC) in Figure 8. The timing loop comprises a second-order PLL (phase-locked loop)

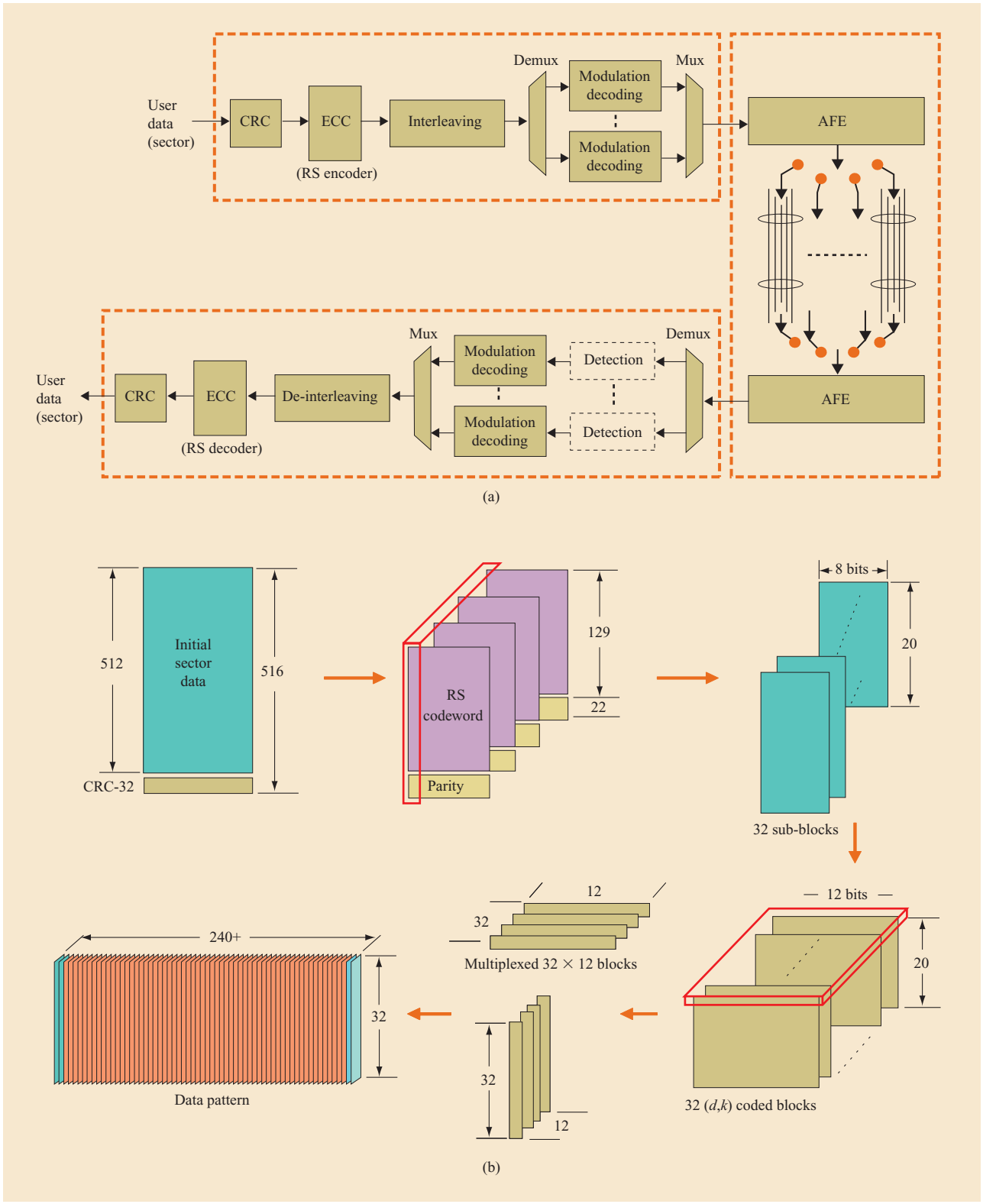

Figure 9

(a) Dataflow architecture. (b) "Write sector" procedure for 512-byte sector. (CRC: cyclic redundancy check; ECC: error-correcting code; RS: Reed–Solomon code; mux: multiplexer; AFE: analog front end; demux: demultiplexer.)

driven by an error signal derived by the deviations of the positions of zero-crossings of the derivative of the readback signal. Finally, the synchronous output of the interpolator is filtered and passed to a binary adaptive-threshold detector to produce estimates of the stored symbols. One of the functions of the digital filter (f_k) in front of the detector is to eliminate rapid dc fluctuations at the detector input by introducing a null at dc. To improve the bit error rate, an additional detector is used in cascade with the threshold detector, which is not shown in the figure. This detector acts on the output of the threshold detector and locates and corrects violations of the d-constraint, that is, the minimum number of 0s between two 1s imposed by the constrained code. In our prototype system, we have used a $d = 1$ code, which implies that a 0 (no indentation) is always enforced between two successive 1s (indentations). As these constraint violations account for the vast majority of errors, a substantial improvement in the bit error rate is obtained.

Dataflow

The dataflow includes all functions related to the host interface, error-correction coding, constrained coding, data format, and data interleaving. It also provides the necessary parameters to the servo controller and in general supervises the complete system functionality. It receives the user data (sectors) and generates the data blocks that are stored in each storage field. The data processing is performed in order to handle the errors (random or bursts) introduced during the write/read operations, reallocate and restructure the data for maximizing the storage efficiency of the device, and adapt the data stored in each storage field to the channel characteristics using a proper constrained coding scheme. As shown in **Figure 9(a)**, during a "write sector" operation, a cyclic redundancy check (CRC) is appended to the initial data, thus enabling the detection of any erroneously reconstructed data block in the receiver. For error correction, a Reed–Solomon (RS) code is used along with proper interleaving. The number of code-words and the parity symbols per code-word determine the total system storage efficiency along with any additional padding. The device reliability is determined by the statistics of the channel errors introduced, the RS code used, and the interleaving scheme applied. The use of a stronger RS code increases reliability but also increases the redundancy introduced, so the storage efficiency decreases. By exploiting the 2D structure of the data probes, a logical organization in small subdevices can be used, and a new interleaving technique has been developed that results in improved reliability for a given RS code and minimization of the additional padding required. A new data-allocation method has also been developed that performs writing of unequal-length data blocks using parallel operating probes [36]. **Figure 9(b)** describes the write sector procedure for a sector of 512 bytes (note that the dataflow supports sector sizes of both 512 and 1,024 bytes). Specifically, the block generated by the user data and the appended CRC is split into a number of data words (determined by the interleaving depth), and each data word is processed by an RS encoder. The generated code-words are interleaved, header and trailer information is appended, and the data blocks stored in each storage field are processed by a (d, k) constrained code encoder. The constrained codes impose restrictions on the number of consecutive 1s and 0s in the encoded data sequence. The code parameters d and k are nonnegative integers, with $k > d$, where d indicates the minimum number of 0s between two 1s, and k indicates the maximum number of zeros between two 1s. For our recording device, the most important constraint is the d-constraint because it determines the distance of consecutive indentations. As mentioned above, we have selected $d = 1$.

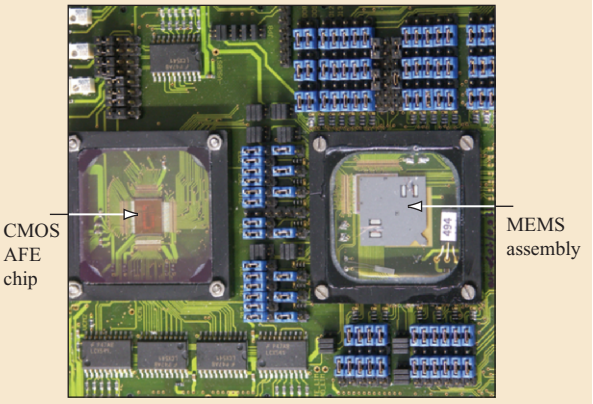

Figure 10

Storage system prototype.

Because the write operation of the device is a type of demultiplexing into the various channels, multiplexing is also performed on the encoded data blocks in order to generate the final write pattern. When the data probes are directly above the proper position in each storage field, this write pattern is used by the AFE circuitry to perform the write operation. The reverse procedure is performed during a "read sector" operation.

Storage system demonstration

A small-scale storage system prototype (shown in **Figure 10**) comprising all of the critical components presented in the previous sections has been built and its

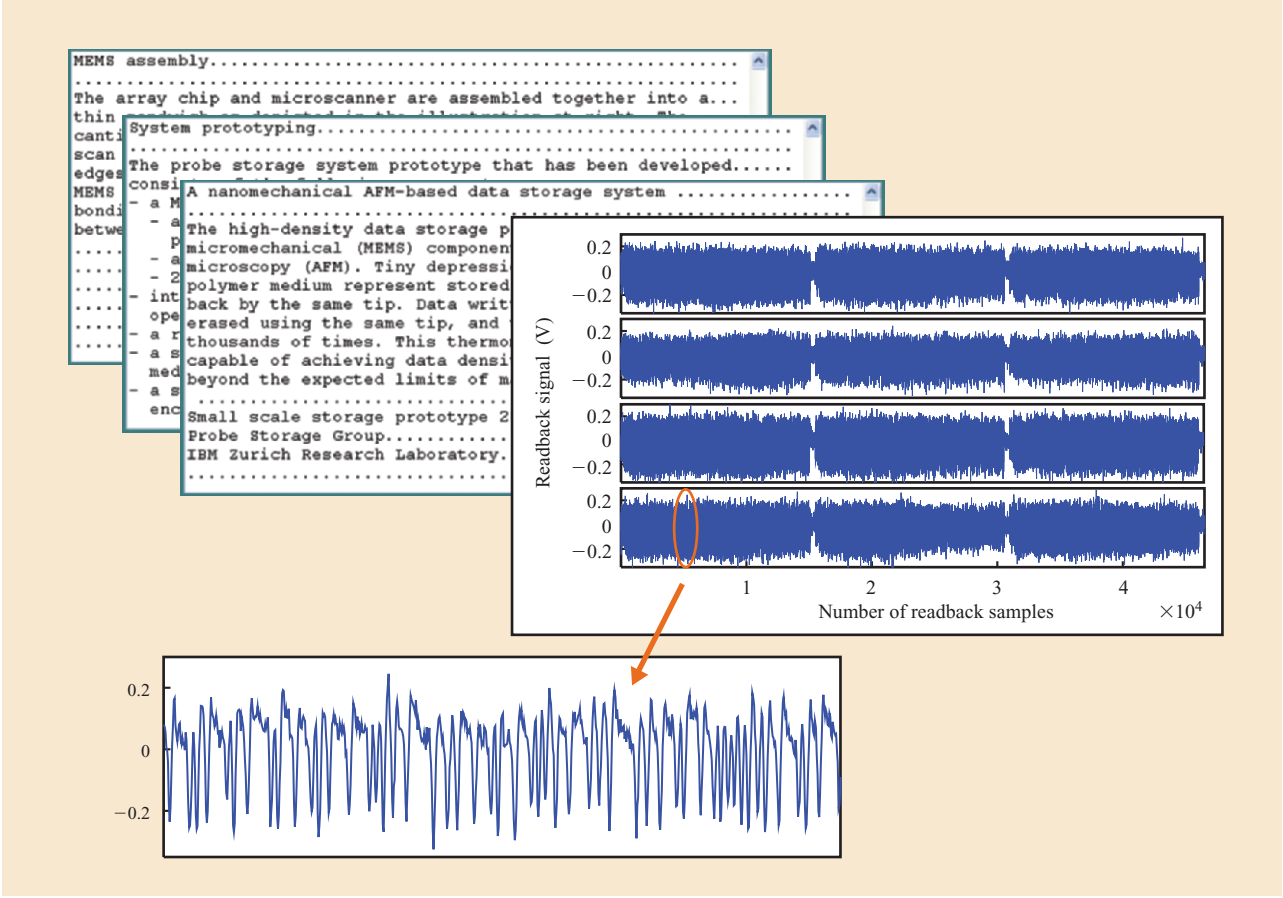

Figure 11

Sector write and read demonstration at 840 Gb/in^2.

functionality experimentally verified. A personal computer was connected through the host interface with the electronics board that hosts the MEMS assembly and the AFE chip. The AFE chip was interconnected by wire bonding to the cantilever array chip. The interface between the AFE electronics and the host PC was implemented in an onboard digital signal processor (DSP) and field-programmable gate array (FPGA) configuration and supports standard read/write sector commands. The system components of the small-scale prototype were implemented on the onboard DSP/FPGA configuration.

Three ASCII files were transformed in three user sectors of 1,024 bytes each. The sectors were processed by all stages of the dataflow presented in the previous section. The resulting symbol sequences were stored in four different data fields occupying three different data tracks in each field. The track size spanned 90 μm in the x-direction, and the distance between adjacent tracks was 32 nm in the y-direction. Each track contained 5,300 symbols, and the distance between adjacent symbols was 16 nm. The resulting effective areal storage density was 840 Gb/in^2. During reading of the stored information, the two-sensor controller presented in the previous section was used to ensure convergence to the track centerline, accurate positioning during the track-follow procedure, and reliable stepping to the subsequent tracks. The readback signals from the levers were processed by the read channel described in the previous section, and the symbols of each track were detected with an error rate of approximately 10^{-4} prior to error-correction coding. After the reverse operation of the dataflow, the complete sector information was recovered from the ECC module. **Figure 11** shows the readback signal from four cantilevers and three different tracks. Each row represents a different cantilever waveform with data from three data tracks. A close-up of a portion of the readback signal shown in the figure demonstrates the recording quality. In Figure 11, the error-free information of the readback sectors is also shown (upper left). This is the first time that an areal

storage density demonstration of 840 Gb/in^2 has been performed with all the building blocks of a storage device.

Conclusion

Ultrahigh densities beyond 1 Tb/in^2 can be achieved by probe-based storage technologies. A small-scale prototype demonstrating all the basic functions of a storage device based on scanning probes has been presented in this paper. Starting from the basic principle of operation all the way to the higher-level system functionality, the building blocks have been described and experimentally characterized. The complete prototype system functionality was verified with experimental results of multiple sectors recorded using multiple levers at 840 Gb/in^2 and read back without errors. This is the first scanning probe-storage technology for which ultrahigh areal density recording and reliable retrieval have been demonstrated using a fully functional storage device prototype.

Although tremendous progress has been made from the initial concept to the building of a fully functional prototype storage system, more technical challenges need to be addressed prior to commercializing such a new technology. These challenges include optimal tradeoff between number of tips, data rate, and power consumption, tracking of more than 1,000 probes at subnanometer resolution, process improvements for controlled cantilever-array homogeneity, further characterization and optimization of tip–medium interaction, and finally, thorough assessment of system-level reliability.

Acknowledgments

We thank our colleagues G. Binnig and P. Vettiger for their pioneering work and initiation of the "Millipede" project. We also thank J. Frommer, B. Miller, J. Mamin, J. Gordon, and T. Magbitang of the IBM Almaden Research Center for their invaluable contributions to the polymer media work. We thank T. Albrecht and J. Windeln for contributions to the progress of the project. Finally, we would like to thank our colleagues P. Seidler and W. Bux for their continued support of this project.

References

1. H. J. Mamin, L. S. Fan, S. Hoen, and D. Rugar, "Tip-Based Data Storage Using Micromechanical Cantilevers," *Sensors & Actuators A* **48**, No. 3, 215–219 (1995).
2. C. F. Quate, "Method and Means of Data Storage Using Tunnel Current Data Readout," U.S. Patent No. 4,575,822, 1986.
3. H. J. Mamin, B. D. Terris, L. S. Fan, S. Hoen, R. C. Barrett, and D. Rugar, "High-Density Data Storage Using Proximal Probe Techniques," *IBM J. Res. & Dev.* **39**, No. 6, 681–700 (1995).
4. H. J. Mamin, R. P. Ried, B. D. Terris, and D. Rugar, "High-Density Data Storage Based on the Atomic Force Microscope," *Proc. IEEE* **87**, No. 6, 1012–1013 (1999).
5. P. Vettiger, G. Cross, M. Despont, U. Drechsler, U. Dürig, B. Gotsmann, W. Häberle, et al., "The 'Millipede'—Nanotechnology Entering Data Storage," *IEEE Trans. Nanotechnol.* **1**, No. 1, 39–55 (2002).
6. E. Eleftheriou, T. Antonakopoulos, G. K. Binnig, G. Cherubini, M. Despont, A. Dholakia, U. Dürig, et al., "Millipede—A MEMS Based Scanning-Probe Data Storage System," *IEEE Trans. Magn.* **39**, No. 2, 938–945 (2003).
7. G. Binnig, H. Rohrer, Ch. Gerber, and E. Weibel, "7×7 Reconstruction on Si(111) Resolved in Real Space," *Phys. Rev. Lett.* **50**, No. 2, 120–123 (1983).
8. G. Binnig, C. F. Quate, and Ch. Gerber, "Atomic Force Microscope," *Phys. Rev. Lett.* **56**, No. 9, 930–933 (1986).
9. S. Gidon, O. Lemonnier, B. Rolland, O. Bichet, C. Dressler, and Y. Samson, "Electrical Probe Storage Using Joule Heating in Phase Change Media," *Appl. Phys. Lett.* **85**, No. 26, 6392–6394 (2004).
10. H. F. Hamann, M. O'Boyle, Y. C. Martin, M. Rooks, and H. K. Wickramasinghe, "Ultra-High-Density Phase-Change Storage and Memory," *Nat. Mater.* **5**, 383–387 (2006).
11. L. R. Carley, J. A. Bain, G. K. Fedder, D. W. Greve, D. F. Guillou, M. S. C. Lu, T. Mukherjee, S. Santhanam, L. Abelmann, and S. Min, "Single Chip Computers with Microelectromechanical Systems-based Magnetic Memory," *J. Appl. Phys.* **87**, No. 9, 6680–6685 (2000).
12. H. Park, J. Jung, D.-K. Min, S. Kim, S. Hong, and H. Shin, "Scanning Resistive Probe Microscopy: Imaging Ferroelectric Domains," *Appl. Phys. Lett.* **84**, No. 10, 1734–1736 (2004).
13. H. J. Mamin and D. Rugar, "Thermomechanical Writing with an Atomic Force Microscope Tip," *Appl. Phys. Lett.* **61**, No. 8, 1003–1005 (1992).
14. H. Pozidis, W. Häberle, D. W. Wiesmann, U. Drechsler, M. Despont, T. Albrecht, and E. Eleftheriou, "Demonstration of Thermomechanical Recording at 641 Gbit/in^2," *IEEE Trans. Magn.* **40**, No. 4, 2531–2536 (2004).
15. D. Wiesmann, U. Dürig, B. Gotsmann, A. Knoll, H. Pozidis, F. Porro, and R. Vecchione, "Ultra-High Storage Densities with Thermo-Mechanical Probes and Polymer Media," *Proceedings of the Innovative Mass Storage Technologies Workshop*, Enschede, The Netherlands, 2007, pp. 19–20; see *http://imst2007.ewi.utwente.nl/imst_program.pdf*.
16. M. Despont, J. Brugger, U. Drechsler, U. Dürig, W. Häberle, M. Lutwyche, H. Rothuizen, et al., "VLSI-NEMS Chip for AFM Data Storage," *Sensors & Actuators A* **80**, 100–107 (2000).
17. M. Despont, U. Drechsler, R. Yu, H. B. Pogge, and P. Vettiger, "Wafer-Scale Microdevice Transfer/Interconnect: Its Application in an AFM-Based Data-Storage System," *J. Microelectromech. Syst.* **13**, No. 6, 895–901 (2004).
18. M. A. Lantz, H. E. Rothuizen, U. Drechsler, W. Häberle, and M. Despont, "A Vibration Resistant Nanopositioner for Mobile Parallel-Probe Storage Applications." *J. Microelectromech. Syst.* **16**, No. 1, 130–139 (2007).
19. B. Gotsmann and U. Dürig, "Nano-Thermomechanics: Fundamentals and Application in Data Storage Devices," *Applied Scanning Probe Methods IV: Industrial Applications*, B. Bhushan and H. Fuchs, Eds., Springer, Berlin, Heidelberg, 2006, pp. 215–250.
20. U. Dürig, "Fundamentals of Micromechanical Thermoelectric Sensors," *J. Appl. Phys.* **98**, No. 4, 044906-1–44906-14 (2005).
21. C. Hagleitner, T. Bonaccio, A. Pantazi, A. Sebastian, and E. Eleftheriou, "An Analog Frontend Chip for a MEMS-Based Parallel Scanning-Probe Data-storage System," *Proceedings 2006 Symposium on VLSI Circuits Digest of Technical Papers*, Honolulu, HI, 2006, pp. 57–58.
22. C. Hagleitner, T. Bonaccio, H. Rothuizen, J. Lienemann, D. Wiesmann, G. Cherubini, J. G. Korvink, and E. Eleftheriou, "Modeling, Design, and Verification for the Analog Front-End of a MEMS-Based Parallel Scanning-

Probe Storage Device," *IEEE J. Solid-State Circuits* **42**, No. 8, 1779–1789 (2007).
23. A. Pantazi, A. Sebastian, G. Cherubini, M. Lantz, H. Pozidis, H. Rothuizen, and E. Eleftheriou, "Control of MEMS-Based Scanning-Probe Data Storage Devices," *IEEE Trans. Control Syst. Technol.* **15**, No. 5, 824–841 (2007).
24. M. A. Lantz, G. K. Binnig, M. Despont, and U. Drechsler, "A Micromechanical Thermal Displacement Sensor with Nanometer Resolution," *Nanotechnology* **16**, 1089–1094 (2005).
25. D. Wiesmann and A. Sebastian, "Dynamics of Silicon Micro-heaters: Modelling and Experimental Identification," *Proceedings of the 19th IEEE International Conference on Micro Electro Mechanical Systems*, Istanbul, Turkey, 2006, pp. 182–185.
26. A. Sebastian, D. Wiesmann, C. Hagleitner, and E. Eleftheriou, "Performance Characteristics of a Thermo-electric Topography Sensor," *IBM Research Report RZ-3696*, 99706, September 25, 2007.
27. B. Gotsmann and U. Dürig, "Thermally Activated Nanowear Modes of a Polymer Surface Induced by a Heated Tip," *Langmuir* **20**, No. 4, 1495–1500 (2004).
28. A. Knoll, P. Bächtold, J. Bonan, G. Cherubini, M. Despont, U. Drechsler, U. Dürig, et al., "Integrating Nanotechnology into a Working Storage Device," *Microelectronic Eng.* **83**, 1692–1697 (2006).
29. B. Gotsmann, U. Dürig, S. Sills, J. Frommer, and C. J. Hawker, "Controlling Nanowear in a Polymer by Confining Segmental Relaxation," *Nano Lett.* **6**, No. 2, 296–300 (2006).
30. H. Pozidis, P. Bächtold, G. Cherubini, E. Eleftheriou, C. Hagleitner, A. Pantazi, and A. Sebastian, "Signal Processing for Probe Storage," *Proceedings of the IEEE International Conference on Acoustics, Speech, and Signal Processing*, Vol. 5, Philadelphia, PA, 2005, pp. 1520–1649.
31. A. Sebastian, A. Pantazi, G. Cherubini, M. Lantz, H. Rothuizen, H. Pozidis, and E. Eleftheriou, "Towards Faster Data Access: Seek Operations in MEMS-Based Storage Devices," *Proceedings of the IEEE International Conference on Control Applications*, Munich, Germany, 2006, pp. 283–288.
32. A. Pantazi, M. Lantz, G. Cherubini, H. Pozidis, and E. Eleftheriou, "Servomechanism for a MEMS-Based Scanning-Probe Data Storage Device," *Nanotechnology* **15**, S612–S621 (2004).
33. A. Sebastian, A. Pantazi, G. Cherubini, E. Eleftheriou, M. Lantz, and H. Pozidis, "Nanopositioning for Probe Storage," *Proceedings of the American Control Conference*, Vol. 6, Portland, OR, June 8–10, 2005, pp. 4181–4186.
34. A. Sebastian, A. Pantazi, and H. Pozidis, "Jitter Investigation and Performance Evaluation of a Small-Scale Probe Storage Device Prototype," *Proceedings of the 50th Annual IEEE Global Telecommunications Conference*, Washington, DC, November 2007, pp. 288–293.
35. A. Pantazi, A. Sebastian, H. Pozidis, and E. Eleftheriou, "Two Sensor Based H∞ Control for Probe Storage," *Proceedings of the 44th IEEE Conference on Decision and Control*, Seville, Spain, 2005, pp. 1174–1179.
36. M. Varsamou and T. Antonakopoulos, "A New Data Allocation Method for Parallel Probe-Based Storage Devices," *IEEE Trans. Magn.* **44**, No. 4, 547–554 (2008).

Received September 21, 2007; accepted for publication October 22, 2007; Internet publication July 23, 2008

Angeliki Pantazi *IBM Research Division, Zurich Research Laboratory, Säumerstrasse 4, 8803 Rüschlikon, Switzerland (agp@zurich.ibm.com)*. Dr. Pantazi received a diploma and Ph.D. degrees in electrical engineering and computer technology from the University of Patras, Greece, in 1996 and 2005, respectively. She is a Research Staff Member at the IBM Zurich Research Laboratory, in Rüschlikon. Her research is focused on probe-based technologies with emphasis on nanopositioning and system-level design for probe-based data-storage devices.

Abu Sebastian *IBM Research Division, Zurich Research Laboratory, Säumerstrasse 4, 8803 Rüschlikon, Switzerland (ase@zurich.ibm.com)*. Dr. Sebastian received a B.E.(Hons.) degree in electrical and electronics engineering from Birla Institute of Technology and Science, Pilani, India, in 1998, and M.S. and Ph.D. degrees in electrical engineering from Iowa State University in 1999 and 2004, respectively. He is currently a Research Staff Member at the IBM Zurich Research Laboratory. His research is primarily focused on the application of control theory to nanoscale devices. He has worked extensively on the analysis of atomic force microscope dynamics and the development of novel modes of operation based on a systems perspective. Currently, he is working on probe-based data storage, focusing on nanopositioning and system-level integration of the various components of the storage device.

Theodore A. Antonakopoulos *Department of Electrical and Computers Engineering, University of Patras, 26500 Rio-Patras, Greece (antonako@upatras.gr)*. Dr. Antonakopoulos received a diploma degree in electrical engineering and a Ph.D. degree from the Department of Electrical Engineering at the University of Patras in 1985 and 1989, respectively. In September 1985, he joined the Laboratory of Electrotechnics, University of Patras, participating in various R&D projects for the Greek Government and the European Union, initially as a Research Staff Member and subsequently as the Senior Researcher of the Communications Group. Since 1991, he has been a faculty member of the Department of Electrical and Computer Engineering, University of Patras, where he is currently a Professor and the Director of the Laboratory of Electrotechnics. From 2001 to 2002, he spent his sabbatical at the IBM Zurich Research Laboratory. His research interests are in the areas of data communications with emphasis on performance analysis, efficient hardware implementation, and rapid prototyping. He has more than 110 publications in these areas and is actively participating in several R&D projects of European industries. Dr. Antonakopoulos is a senior member of the IEEE and a member of the Technical Chamber of Greece.

Peter Bächtold *IBM Research Division, Zurich Research Laboratory, Säumerstrasse 4, 8803 Rüschlikon, Switzerland (peb@zurich.ibm.com)*. Mr. Bächtold received a diploma degree as an Electronics and Telecommunications Technician in 1970. He joined the IBM Zurich Research Laboratory in 1977. Presently, his work as Senior Engineer concentrates on electronic circuit design for probe-based technologies and nanopositioning.

Anthony R. (Tony) Bonaccio *IBM Systems and Technology Group, 1000 River Road, Essex Junction, Vermont 05452 (tb@us.ibm.com)*. Mr. Bonaccio is a Distinguished Engineer at the IBM microelectronics facility in Essex Junction, Vermont. Since joining the analog and mixed-signal design group at IBM in 1979, he has been responsible for the design and development of a wide variety of analog integrated circuit products. His main focus has been on integrated circuits for hard disk drives, including custom interface driver chips, phase-locked loop chips, and low-noise

preamplifiers for magnetoresistive heads. From 1993 to 2001, he was a technical team leader for the development of CMOS and BiCMOS partial-response, maximum likelihood (PRML) data channel chips for use in IBM mobile and consumer hard disk drives. His current assignments include high-speed serial interface and data converter cores for IBM microprocessors and ASICs, as well as the Millipede analog front-end and lever modeling effort. Mr. Bonaccio holds a B.S. in electrical engineering from the University of Rochester, New York, and an M.S. in electrical engineering from the University of Vermont. He holds 35 U.S. patents in the area of analog integrated circuit design and has 17 pending. He is a Senior Member of the IEEE and an Adjunct Professor of Electrical and Computer Engineering at the University of Vermont, where he has offered graduate-level courses in MOS and bipolar analog circuit design since 1988.

Jose Bonan *IBM Research Division, Zurich Research Laboratory, Säumerstrasse 4, 8803 Rüschlikon, Switzerland (bon@zurich.ibm.com).* Mr. Bonan received M.S. degrees in material science from Orsay University (Paris, France) and in electrical engineering from Pierre et Marie Curie University (Paris, France) in 1999 and 2003, respectively. In 1999, he was invited to Lawrence Berkeley National Laboratory as a visiting scholar for one year. He currently is a predoctoral student at the IBM Zurich Research Laboratory, working toward the Ph.D. degree in electronic engineering at the Pierre et Marie Curie University, Paris, France. His main research interests are in analog and mixed-signal integrated circuit design and analog design automation.

Giovanni Cherubini *IBM Research Division, Zurich Research Laboratory, Säumerstrasse 4, 8803 Rüschlikon, Switzerland (cbi@zurich.ibm.com).* Dr. Cherubini received a Laurea degree in electrical engineering (*summa cum laude*) from the University of Padova, Italy, and M.S. and Ph.D. degrees in electrical engineering from the University of California, San Diego. He joined the research staff of IBM in 1987. His research interests include high-speed data transmission and data storage systems. He was coeditor of the 100BASE-T2 Standard for Fast Ethernet transmission over voice-grade cables. More recently, he contributed to the realization of the first fully functional atomic force microscope-based data-storage prototype system. Dr. Cherubini was a co-recipient of the 2003 IEEE Communications Society Leonard G. Abraham Prize Paper Award. He is Fellow of the IEEE and Distinguished Lecturer of the IEEE Communications Society.

Michel Despont *IBM Research Division, Zurich Research Laboratory, Säumerstrasse 4, 8803 Rüschlikon, Switzerland (dpt@zurich.ibm.com).* Dr. Despont received a degree in microtechnology from the Swiss Federal Institute of Technology of Lausanne in 1993 and a Ph.D. degree in physics from the Institute of Microtechnology, University of Neuchatel, Switzerland, in 1996, with a dissertation on the microfabrication of electron microlenses for a miniaturized electron microscope. After a postdoctoral fellowship at the IBM Zurich Research Laboratory in 1996, where he worked on the development of various cantilever-based sensors and pioneered the process development of an ultrathick, high-aspect-ratio UV resist called *SU-8*, he spent one year as a visiting scientist at the Seiko Instrument Research Laboratory in Japan. Since returning to the IBM Zurich Research Laboratory, his work has focused on the development of micromechanical and nanomechanical devices as well as on 3D microdevice integration for system-on-a-chip (SoC) applications.

Richard A. DiPietro *IBM Almaden Research Center, 650 Harry Road, San Jose, CA 95120 (dipietro@almaden.ibm.com).* Dr. DiPietro earned a B.S. degree at the State University of New York at Binghamton in 1976, an M.S. degree in organic chemistry at the University of California, San Diego in 1980, and a Ph.D. degree in synthetic medicinal chemistry at the University of Michigan in Ann Arbor in 1984. Upon completion of a postdoctoral fellowship at Syntex Research, he moved to E. R. Squibb & Sons in New Brunswick, New Jersey, in 1985. He joined the Polymer Science and Technology department at the IBM Almaden Research Center in 1988 as a member of the Synthetic Development Laboratory, where he is currently a Senior Scientist. His interests are the syntheses of monomers, polymers, and assorted organic materials of interest to the electronics industry.

Ute Drechsler *IBM Research Division, Zurich Research Laboratory, Säumerstrasse 4, 8803 Rüschlikon, Switzerland (dre@zurich.ibm.com).* Ms. Drechsler is a Processing Engineer in the Science and Technology department of the IBM Zurich Research Laboratory. She originally joined the IBM Plant in Sindelfingen, Germany, in 1983, while also receiving training in chemical engineering. After this, she worked in the fabrication line for multilayer ceramic packaging, where she was promoted to section head in 1993. In 1996, she joined the Micro/Nanomechanics group at the Zurich Research Laboratory, working on silicon micromachining and processing techniques for probe-based storage array chips and processing-related work for other department projects. She is currently responsible for the organization and operation of the department cleanroom.

Urs Dürig *IBM Research Division, Zurich Research Laboratory, Säumerstrasse 4, 8803 Rüschlikon, Switzerland (drg@zurich.ibm.com).* Dr. Dürig received a degree in experimental physics and a Ph.D. degree, both from the Swiss Federal Institute of Technology, Zurich, Switzerland, in 1979 and 1984, respectively. He was a postdoctoral fellow at the IBM Zurich Research Laboratory, working on near-field optical microscopy in Dieter Pohl's group. In 1986, he became a Research Staff Member and worked in the field of scanning tunneling and force microscopy, investigating metallic adhesion, growth morphology of magnetic thin films, and surface melting. In 1997, he joined the Probe Storage Group at IBM, working on the polymer media development.

Bernd Gotsmann *IBM Research Division, Zurich Research Laboratory, Säumerstrasse 4, 8803 Rüschlikon, Switzerland (bgo@zurich.ibm.com).* Dr. Gotsmann studied physics at the University of Münster, Germany, and the University of York, United Kingdom. In 2000, he received a Ph.D. degree in physics for his work on force detection using dynamic force microscopy. From 2001 to 2006, he was a postdoctoral fellow and a visiting scientist in the Micromechanics/Nanomechanics group of the IBM Zurich Research Laboratory, working on polymer media design and endurance issues in thermomechanical data storage. Since 2006, he has been a Research Staff Member at IBM. His current research activities are in the fields of nano-tribology, nanoscale heat transfer, and polymer design for thermomechanical applications.

Walter Häberle *IBM Research Division, Zurich Research Laboratory, Säumerstrasse 4, 8803 Rüschlikon, Switzerland (wha@zurich.ibm.com).* Mr. Häberle is a development engineer in the Science and Technology department of the IBM Zurich Research Laboratory. In 1974, he joined the IBM Semiconductor Plant in Sindelfingen, Germany, for his education as physics technician and was later promoted to group leader in the Quality Control department of the semiconductor line. In 1987, he joined the IBM Physics Group of Professor G. K. Binnig at the University

of Munich, Germany, where he contributed to the development of atomic force microscopes (AFMs) for applications in a liquid environment for investigating living cells. In 1995, he transferred to the IBM Zurich Research Laboratory, where he was responsible for prototyping a new low-cost AFM instrument. Since 1997, he has been involved in various aspects of the probe-based data-storage project. In 2003, he spent a sabbatical year at the Wayne State University in Detroit, Michigan, where he investigated heat-transfer rates in biological samples using thermomechanical lever technologies. Since 2006, the focus of his research has been on the tape path of tape drive systems.

Christoph Hagleitner *IBM Research Division, Zurich Research Laboratory, Säumerstrasse 4, 8803 Rüschlikon, Switzerland (hle@zurich.ibm.com).* Dr. Hagleitner obtained a diploma degree and a Ph.D. degree in electrical engineering from the Swiss Federal Institute of Technology (ETH), Zurich, in 1997 and 2002, respectively. After receiving his Ph.D. degree in 2002 with a thesis on a CMOS single-chip gas detection system, he headed the circuit design group of the Physical Electronics Laboratory at the ETH Zurich. In 2003, he joined the IBM Zurich Research Laboratory in Rüschlikon, Switzerland, where he works on the analog front-end design and system aspects of a novel probe-storage device.

James L. Hedrick *IBM Almaden Research Center, 650 Harry Road, San Jose, California 95120 (hedrick@almaden.ibm.com).* Dr. Hedrick received B.S. and Ph.D. degrees from the Virginia Tech in 1981 and 1985, respectively, under the mentorship of Dr. James E. McGrath. He is currently a Research Staff Member at the IBM Almaden Research Center, and he is an investigator in the NSF Center for Polymeric Assemblies and Macromolecular Interfaces. He was the recipient of the 2003 American Chemical Society (ACS) Carl S. Marvel Creative Polymer Chemistry Award and the 2006 ACS Industrial Sponsors Award. His research has focused on new synthetic methodologies for microelectronics, nanotechnology, and biocompatible materials using organic catalysis.

Daniel Jubin *IBM Research Division, Zurich Research Laboratory, Säumerstrasse 4, 8803 Rüschlikon, Switzerland (dju@zurich.ibm.com).* In 1993, Mr. Jubin received an engineering degree in Optronics from L'École Nationale Supérieur des Sciences Appliquées et de Technologie in Lannion, France. Until 1997, he worked for a spinoff of the Swiss Federal Institute of Technology of Zurich, developing an all-solid-state laser for ultrashort pulse generation. He then joined JDS-Uniphase, where he participated in developing high-power pump laser diodes for erbium-doped fiber amplifiers. In 2001, he joined the silicon-oxynitride waveguide effort in the IBM Zurich Research Laboratory, where he was in charge of characterizing integrated optical compounds. He moved to the Microfabrication and Nanofabrication group in 2003 and, since then, has been responsible for the characterization of MEMS chips.

Armin Knoll *IBM Research Division, Zurich Research Laboratory, Säumerstrasse 4, 8803 Rüschlikon, Switzerland (ark@zurich.ibm.com).* Dr. Knoll received an M.S. degree in experimental physics from the University of Würzburg, Germany (1998), and a Ph.D. degree in physical chemistry from the University of Bayreuth, Germany, in 2004. During his education, he specialized in scanning probe methods in various environments. In a postdoctoral fellowship with the University of Basel for 15 months (2003/2004), he worked on functional MEMS structures produced by two photon polymerization lithography. After a visiting scientist position from 2005 to 2006, he became Research Staff Member at the Zurich Research Laboratory in April 2006. As a member of the Advanced Media Concepts group of the probe-storage project, he is currently working on optimizing polymeric media for storage applications.

Mark A. Lantz *IBM Research Division, Zurich Research Laboratory, Säumerstrasse 4, 8803 Rüschlikon, Switzerland (mla@zurich.ibm.com).* Dr. Lantz received B.Sc. and M.Sc. degrees in electrical engineering from the University of Alberta, Canada, in 1991 and 1993, and a Ph.D. degree from the University of Cambridge, United Kingdom, in 1997 for work in the field of scanning probe microscopy. He then spent two years as a postdoctoral researcher at the Joint Research Center for Atom Technology in Japan, investigating the application of scanning probes in biophysics, followed by two years of research in the area of low-temperature scanning force microscopy at the Physics Institute in University of Basel, Switzerland. In 2001, he joined the Micromechanics/Nanomechanics group of the IBM Zurich Research Laboratory as a Research Staff Member. His current research activities are focused on micromechanical and nanomechanical devices and systems for scanning-probe-based data storage, tribology, and magnetic tape drive technology.

John Pentarakis *Department of Electrical and Computer Engineering, University of Patras, 26500 Rio-Patras, Greece (ipentarakis@upatras.gr).* Mr. Pentarakis received his engineering diploma from the department of electrical and computer engineering at the University of Patras, Greece, in 2004. In September 2004, he joined the Laboratory of Electrotechnics, University of Patras, as a research staff member, participating in various R&D projects for the Greek government and the industrial sector in the fields of data communications and embedded systems. Currently, he is a post-graduate student at the University of Patras, and his research interests are in the areas of digital communications with emphasis on signal detection and coding.

Haralampos Pozidis *IBM Research Division, Zurich Research Laboratory, Säumerstrasse 4, 8803 Rüschlikon, Switzerland (hap@zurich.ibm.com).* Dr. Pozidis received a diploma degree in computer engineering and informatics from the University of Patras, Greece, in 1994, and the M.Sc. and Ph.D. degrees in electrical engineering from Drexel University, Philadelphia, Pennsylvania, in 1997 and 1998, respectively. From 1998 until 2001, he was with Philips Research (Eindhoven, The Netherlands), where he worked on read channel design for optical storage devices, in particular DVD and Blu-ray** disc formats, with focus on channel modeling, equalization, and bit detection. Since 2001, he has been with the IBM Zurich Research Laboratory, working on basic recording technology, signal processing, and overall system design for MEMS-based scanning-probe data-storage devices.

Russell C. Pratt *IBM Research Division, IBM Almaden Research Center, 650 Harry Road, San Jose, California 95120 (rcpratt@us.ibm.com).* Dr. Pratt received his B.Sc. degree in chemistry from the University of British Columbia, Canada, in 1998 and his Ph.D. degree in chemistry from Stanford University, California, in 2004. He then spent one year as a joint Stanford–IBM postdoctoral researcher before becoming a supplemental IBM employee in the Advanced Organic Materials group in 2005.

Hugo Rothuizen *IBM Research Division, Zurich Research Laboratory, Säumerstrasse 4, 8803 Rüschlikon, Switzerland (rth@zurich.ibm.com)*. Dr. Rothuizen studied physics at the Swiss Federal Institute of Technology, Lausanne, completing his Ph.D. degree in 1994 with a dissertation on selective-area epitaxial growth of III–V materials. Since becoming a Research Staff Member at the IBM Zurich Research Laboratory in 1996, he has worked on the patterning of nanometer-scale structures and on the design of micromechanical sensors and actuators. He is currently involved in the modeling of MEMS devices and in the development of packaging solutions.

Richard Stutz *IBM Research Division, Zurich Research Laboratory, Säumerstrasse 4, 8803 Rüschlikon, Switzerland (ris@zurich.ibm.com)*. Mr. Stutz is a senior technical specialist in the Micromechanics/Nanomechanics group of the IBM Zurich Research Laboratory, which he joined in 1998. His current technical responsibilities and interests include electroplating, plasma sputter deposition, MEMS fabrication, surface modification by stamping techniques, and focused ion beam machining for micromechanical devices. Prior to joining IBM, he was responsible for the fabrication technological aspect of holography, electroplating, injection molding, stamping, integrated and micro-optical systems as a member of the technical staff of the Paul Scherrer Institute, and the Centre Suisse d'Electronique et de Microtechnique in Zurich, Switzerland.

Maria Varsamou *IBM Research Division, Zurich Research Laboratory, Säumerstrasse 4, 8803 Rüschlikon, Switzerland (vma@zurich.ibm.com)*. Ms. Varsamou received a diploma degree in electrical and computer engineering from the University of Patras, Greece, in 2000. After this, she became a graduate student at the same department in the Laboratory of Electrotechnics. She is currently with the IBM Zurich Research Laboratory, in Rüschlikon, Switzerland, working on probe-based data storage, with emphasis on error control coding.

Dorothea Wiesmann *IBM Research Division, Zurich Research Laboratory, Säumerstrasse 4, 8803 Rüschlikon, Switzerland (dor@zurich.ibm.com)*. In 2000, Dr. Wiesmann received a Ph.D. degree from the Swiss Federal Institute of Technology, Zurich, Switzerland, in 2000 for work in the field of planar optical waveguides. In 2000, she became a Research Staff Member with the Photonic Networks group, IBM Research, Zurich Research Laboratory. In 2002, she joined the Micromechanics/Nanomechanics group and since then has been working on scanning-probe-based data storage, focusing primarily on performance during extended storage operation and optimization of the probe design with respect to power consumption and data rate.

Evangelos Eleftheriou *IBM Research Division, Zurich Research Laboratory, Säumerstrasse 4, 8803 Rüschlikon, Switzerland (ele@zurich.ibm.com)*. Dr. Eleftheriou received a B.S. degree in electrical engineering from the University of Patras, Greece, in 1979, and M.Eng. and Ph.D. degrees in electrical engineering from Carleton University, Ottawa, Canada, in 1981 and 1985, respectively. He joined the IBM Zurich Research Laboratory in 1986, where he worked on various projects related to transmission technology, magnetic recording, and probe storage. He currently manages the advanced storage technologies group. In 2005, Dr. Eleftheriou was co-recipient of the Eduard Rhein Technology Award. He was co-recipient of the 2003 IEEE Communications Society Leonard G. Abraham Prize Paper Award. In January 2002, he was elected Fellow of the IEEE, and in 2005, he became an IBM Fellow and was elected to the IBM Academy of Technology.